

# Distributed Gradient Descent in Bacterial Food Search

Shashank Singh<sup>\*1</sup>, Sabrina Rashid<sup>\*2</sup>, Zhicheng Long<sup>3</sup>, Saket Navlakha<sup>4</sup>, Hanna Salman<sup>5</sup>, Zoltán N. Oltvai<sup>6</sup>, Ziv Bar-Joseph<sup>7†</sup>

<sup>1</sup> Machine Learning Department and Department of Statistics, Carnegie Mellon University, Pittsburgh, PA 15213.

<sup>2</sup> Computational Biology Department, Carnegie Mellon University, Pittsburgh, PA 15213.

<sup>3</sup> Department of Pathology, Department of Physics and Astronomy, University of Pittsburgh, Pittsburgh, PA 15213.

<sup>4</sup> The Salk Institute for Biological Studies, Center for Integrative Biology, La Jolla, CA 92037.

<sup>5</sup> Department of Physics and Astronomy, Department of Computational and Systems Biology, University of Pittsburgh, Pittsburgh, PA 15260.

<sup>6</sup> Department of Pathology, Department of Computational and Systems Biology, University of Pittsburgh, Pittsburgh, PA 15260.

<sup>7</sup> Machine Learning Department and Computational Biology Department, Carnegie Mellon University, Pittsburgh, PA 15213.

\* These authors contributed equally.

† Contact author. Email: zivbj@cs.cmu.edu

**Abstract.** Communication and coordination play a major role in the ability of bacterial cells to adapt to ever changing environments and conditions. Recent work has shown that such coordination underlies several aspects of bacterial responses including their ability to develop antibiotic resistance. Here we develop a new distributed gradient descent method that helps explain how bacterial cells collectively search for food in harsh environments using extremely limited communication and computational complexity. This method can also be used for computational tasks when agents are facing similarly restricted conditions. We formalize the communication and computation assumptions required for successful coordination and prove that the method we propose leads to convergence even when using a dynamically changing interaction network. The proposed method improves upon prior models suggested for bacterial foraging despite making fewer assumptions. Simulation studies and analysis of experimental data illustrate the ability of the method to explain and further predict several aspects of bacterial swarm food search.

Supporting movies: [https://www.andrew.cmu.edu/user/sabrinar/Bacteria\\_movies/](https://www.andrew.cmu.edu/user/sabrinar/Bacteria_movies/)

## Introduction

There are many parallel requirements of computational and biological systems, suggesting that each can learn from the other. Like virtually all large-scale computing platforms, biological systems are mostly distributed consisting of molecules, cells, or organisms that interact, coordinate, and reach decisions without central control [1], [2]. However, unlike most computational methods, biological systems rely on very limited communication protocols, do not assume that the identity of the communicating agents is known and only utilize simple computations [3]. This makes biological systems more resilient to environmental noise and allows them to function efficiently in harsh settings, a property that is desirable in computational systems as well (for example, sensor networks in remote locations or robot swarms in mines [4]). Recent work demonstrated that for certain network based distributed algorithms, our improved ability to study biological processes at the molecular and cellular levels allows us to both, improve our understanding of these biological processes and suggest novel ways to improve distributed computational algorithms [5].

For example, a number of key machine learning optimization algorithms, including neural networks and non-negative matrix factorization, have been inspired by information processing in the brain [6], [7]. Here we show that a variant of a commonly used machine learning coordination algorithm, *distributed gradient descent (DGD)*, can be used to explain how large bacterial swarms efficiently search for food. Similar to the regular gradient descent setting [8], [9], by sensing the food gradient, each cell has its own belief about the location of the food source (Figure 1a). However, given potential obstacles in the environment, as well as limits on the ability of each cell to accurately detect and move toward the food source in this environment, the individual trajectories may not produce the optimal path to the food source. Thus, in addition to using their own belief each cell also sends and receives messages from other cells (either by secreting specific signaling molecules or by physical interaction; Figure 1(b)), which it then integrates to update its own belief and determine subsequent movement direction and velocity. The process continues until the swarm converges to the food source.

While it is possible to observe that the group-based approach shortens the time it takes a single cell to reach the food source (both experiments and simulations as we show below), and several aspects of the molecular pathways involved in the communication between bacterial cells have

been studied [10], the *computations* that the cells perform have not been well characterized. Current models [11],[12] are largely based on differential equation methods. While these can indeed lead to a fast, coordinated search, they do not fully take into account the dynamically changing topology of cells' interaction network over time. Furthermore, they make unrealistically strong assumptions about the abilities of cells to identify the source(s) of the messages and to utilize a large (effectively continuous valued) set of messages, which is unrealistic given the limited computational powers bacteria cells possess.

Here, we introduce a distributed gradient descent (DGD) model that makes biologically realistic assumptions regarding the dynamics of the agents, the size of the set of the messages, and the agents' ability to identify senders. We show that our DGD model solves the bacterial food search problem more efficiently (in terms of the overall complexity of messages sent) and more quickly (in terms of the time it takes the swarm to reach the food source) when compared to current differential equation models and also leads to better agreement with experimental results. We argue that our model is in fact a distributed pseudogradient descent method,<sup>1</sup> and hence we can adapt proof by [13] to show that our model converges to a local minimum under reasonable assumptions on how bacteria communicate. Simulation studies indicate that the solution is feasible and leads to improvements over prior methods and over single cell and single swarm behavior. Finally, we discuss how these efficient and robust bacterial algorithms may be applicable to distributed sensors or wireless networks that operate under strict communication and computation constraints [2], [14].

## Results

### A computational framework for understanding bacterial food search

While bacterial food search has been extensively studied, at both molecular and cellular levels, most studies have focused on the individual cell, rather than characterizing the collective performance of a bacterial swarm. To formally analyze this process and to derive methods that can be used for other tasks performed by severely restricted agents, we consider collective bacterial

---

<sup>1</sup> *pseudogradient* here refers to the fact that each agent's *expected* direction of movement at each time step is a descent direction, even though it may not be a descent direction in actuality due to stochasticity.

food search as a distributed gradient descent (DGD) algorithm for determining the direction of movement for each agent. DGD is a classic distributed optimization algorithm for finding a minimum of an objective function. In our case, the minimum corresponds to the food source, and the objective function incorporates the terrain over which the bacteria cells search. DGD is based on *message passing* between nodes (individual cells or agents) in a graph. These messages contain information that each node uses to update its own movement direction and velocity. The goal of DGD is for all nodes to converge to a single location in the search space.

While DGD has been studied in several different application areas, there are several differences between standard DGD algorithms [15,16] and bacterial food search. First, classical algorithms assume that message passing occurs on a fixed and static network, whereas for bacteria edges and their weights are based on a sphere of influence which changes over time based on each bacterium's current location. Second, classical algorithms typically do not limit message complexity (in terms of message size and number of messages sent), whereas bacteria have a limited message vocabulary [3] and may attempt to minimize the number of messages sent to conserve energy. Third, classical algorithms require significant data aggregation at individual nodes, whereas bacteria are not believed to collect and store data in this way. Considering that bacteria have been solving this optimization problem under these constraints for billions of years, we hope to learn interesting algorithmic strategies from studying this process. Such algorithms may address a new class of problems that may be important in other applications, such as swarm robotics [18].

For bacteria, the movement of an agent  $i$  at time  $n$  is a function  $d_i(n)$  of two quantities: its own sense of direction  $\theta_i(n)$  (based on the chemical gradient), and the locations and movement directions of other cells in the swarm. Nodes in this graph correspond to bacteria, at some current location  $\mathbf{x}_i(n)$  and edges, representing physical distance, exist between two bacteria that lie within a sphere of influence of each other. The challenge lies in updating  $d_i(n)$  based on the individual belief and the beliefs of neighbors, while using simple messaging (formalized below). For bacteria, messages passed along edges in the graph contains both homophilic components (attraction and orientation) and a heterophilic component (repulsion). Below, we first present prior work by Shklarsh et al. [12] that describes bacteria food search using a differential equation (DE) model

and then present our DGD model, which improves upon the Shklarsh DE model in performance while relying on weaker, more biologically realistic, assumptions.

### The Shklarsh model: Cell based differential equation computation

Initial models for bacterial swarm movements assume that cells solve a system of differential equations (DE) to determine their next move [12]. We briefly review this model below. The model assumes that individual cells follow a chemical gradient of food source by decreasing their (random) tumbling frequency at high concentrations and thus largely move in the direction of the food. Specifically, the bacteria perpetually moves in a direction which it repeatedly perturbs randomly. The frequency and magnitude of these perturbations are inversely related to the change in the food concentration between iterations, with the rough effect that the agent continues to move in directions along the gradient. Formally, under these assumptions, at time  $n$ , the bacterium changes its direction by an angle  $\theta(n)$ , which is a function of  $\Delta c(n)$ , the difference in food concentration between the current and previous time steps. Specifically, the new tumbling angle  $\theta(n)$  is sampled randomly from a Gaussian distribution  $\theta(n) \sim N(\theta(n - \Delta n), \sigma(\Delta c(n))^2)$  centered at the previous angle  $\theta(n - \Delta n)$ , with the variance  $\sigma(\Delta c(n))^2$  given as:

$$\sigma(\Delta c(n))^2 = \begin{cases} 0; & \Delta c(n) \geq 0 \\ \pi; & \Delta c(n) < 0 \end{cases}. \quad (1)$$

Thus, based only on its own perception of the food gradient, the  $i^{th}$  agent updates its location  $\mathbf{x}_i(n)$  according to

$$\mathbf{x}_i(n + \Delta n) = \mathbf{x}_i(n) + \mathbf{v}_i(n) \cdot \Delta n, \quad (2)$$

where  $\mathbf{v}_i(n)$  is the unit vector in the direction of the movement.

$$\mathbf{v}_i(n) = (\cos(\theta(n)), \sin(\theta(n))). \quad (3)$$

So far we have discussed movements based on sensing by individual cells (agents). However, in almost all cases, cells move in large swarms. Communication among swarm members, and between swarms, improves the ability of individual cells to handle obstacles in the direction of

the food source leading to faster and more efficient ways to reach the food. The communication among agents is divided into three components: (1) *repulsion* from very close agents to avoid collision ; (2) *orientation* to match the direction of neighboring cells, and (3) *attraction* to distant agents to keep the swarm unified (Figure 1(b)). The model of Shklarsh et al. assumes that cells align their trajectory with the direction of the other cells if they are close enough, while being attracted toward cells that are relatively far away.

Denote by  $\mathbf{u}_i(n)$  the vector agent  $i$  computes using the messages from the other cells (in this model, movements are of fixed length and so the only variable in each iteration is the direction). Then, if any other agents  $j$  are within the physical interaction (repulsion) range  $RR$  as shown in Figure 1(b), the Shklarsh model sets:

$$\mathbf{u}_i(n) = - \sum_{j \in B_{RR}} \frac{\mathbf{x}_i(n) - \mathbf{x}_j(n)}{\|\mathbf{x}_i(n) - \mathbf{x}_j(n)\|}. \quad (4)$$

Otherwise, the Shklarsh model sets:

$$\mathbf{u}_i(n) = \sum_{j \in B_{RO}} \mathbf{v}_j(n) + \sum_{j \in B_{RA}, j \notin B_{RO}} \frac{\mathbf{x}_i(n) - \mathbf{x}_j(n)}{\|\mathbf{x}_i(n) - \mathbf{x}_j(n)\|}, \quad (5)$$

where the first sum is over all agents  $j$  in the orientation range  $RO$  and the second sum is over all agents in the attraction range  $RA$  (but not in the range  $RO$ ). Next, the agent combines the messages it received with its own observation, resulting in the following modification of equation (2):

$$\mathbf{x}_i(n + \Delta n) = \mathbf{x}_i(n) + \left( \frac{\mathbf{u}_i(n)}{\|\mathbf{u}_i(n)\|} + w\mathbf{v}_i(n) \right) \cdot \Delta n, \quad (6)$$

where  $w$  is a scalar weighting factor.

## A distributed gradient descent model

While the model presented by Shklarsh et al. [12] captures the basics of bacterial swarm movements, it suffers from several problems which make it unlikely to be used by real cells and, as we show in Results, less efficient. First, the model assumes that cells can determine their exact distances from *each* other cell (as can be seen by the summations over neighbors cells in the ori-

entation and attraction ranges). This implicitly assumes that cells can *identify* individual senders, which is very unlikely given the large and dynamic nature of bacterial swarms. In addition, the model assumes that cells can interpret complex (real-valued) messages regarding the locations and orientation of other cells, which is also unrealistic [3]. Finally, the model assumes that, within each of the ranges above, each cell exerts the same influence regardless of their distance from the receiving cell, which is again unrealistic due to the nature of the communication channel (diffusion of a secreted protein). We have thus modeled bacterial food search using a DGD model that relaxes many of these assumptions while still allowing cells to (probably) reach an agreement regarding the direction of movement and eventually the location of the food source, as observed in nature.

Our model still distinguishes between physical interactions (leading to repulsion) and messages (secreted proteins). The former is handled by summing up the number of cells that are in physical proximity without relying on their exact location. However, we make several changes to Equation (5). First, we remove the requirement that cells identify the distance and direction to each other cell (and thus determine whether to use the attraction or orientation terms). Instead, we simply sum over all cells, taking into account their relative influences under the assumption that message strength decays exponentially with distance [19]. Second, we discretize the messages that cells receive, resulting in simple messages with finitely many possible values. The changes lead to the following modification of equation (5):

$$\mathbf{u}_i(n) = D_{L,T} \left( \sum_j \exp(-(C_o \|\mathbf{x}_i(n) - \mathbf{x}_j(n)\|)) \mathbf{v}_j(n) + \sum_j \frac{\exp(-(C_a \|\mathbf{x}_i(n) - \mathbf{x}_j(n)\|)) (\mathbf{x}_i(n) - \mathbf{x}_j(n))}{\|\mathbf{x}_i(n) - \mathbf{x}_j(n)\|} \right). \quad (7)$$

Here,  $D_{L,T}$  is a discrete thresholding operator parametrized by  $L$ , a positive integer denoting the number of possible messages, and  $T$ , an upper bound above which all messages are treated as the highest value possible (see [20] for the exact construction of this “stone-age computing” threshold which has been used in ant models).  $C_a$  and  $C_o$  are positive diffusion constants, determining how quickly the attraction and orientation signals diffuse from the source agent. Typically,  $C_o > C_a$ , in which case nearby agents are influenced more by the orientation component and far away agents are influenced more by the attraction component. Under this model, bacteria communicate orientation and attraction information using only  $3 + \log_2 L$  bits to communicate ( $\log_2 8$  bits for direction and  $\log_2 L$  bits for magnitude). In addition, we also add a Gaussian noise component with a small variance  $\sigma$  to make this process stochastic. Note that the individual component of

the agents' movement (based on the chemical gradient they perceive) is identical to that of the Shklarsh model, and that we are modifying only the communication model. See Supplement for the complete combined model.

### **Convergence theorem**

Unlike standard distributed gradient descent algorithms, the model described above does not rely on a fixed network. Instead, in each iteration, the topology of the network (and thus the weights placed on neighbors) changes with their movement. To prove that using such network (and the computation we assume) indeed leads to convergence of the swarm as seen in nature (regardless of agents' starting locations), we adapt a convergence theorem for distributed pseudogradient descent from [13]. The convergence proof is only focused on the attraction component of the model (see Discussion). However, the theorem holds for both synchronous and asynchronous settings, and thus our model could be generalized to the case where agents' messages themselves travel stochastically.

The convergence theorem is fully stated and proven in the Supplement. The main idea of the proof is that there exists a sequence  $\{y(n)\}_{n=1}^{\infty}$  such that, if, at time  $n$ , all agents were to cease to follow the gradient while continuing to move according to the attraction term (i.e., weighted averaging), then all agents would converge to location  $y(n)$ . For example, in the case that all agents communicate with equal weights,  $y(n)$  is simply the mean of the agents' positions at time  $n$ . Under reasonable assumptions on the edge weights, information from each agent is likely to propagate throughout the swarm and so the agents will converge on  $y(n)$  (plus individual noise), regardless of their starting position. Furthermore, once the agents are sufficiently close, the change in  $y(n)$  (which is a weighted average of the gradients perceived by each agent) in each iteration becomes approximately proportional to  $J(y(n))$ , so that the swarm collectively behaves as a traditional gradient descent.

The proof relies on two lemmas stated in the Supplement. The first claims that agents continue move in the correct descent direction once they have detected an increase in food gradient in one of their tumbles (until that direction ceases to be a descent direction). As we show, to achieve such expected decrease as required by the lemma for each step, we need to change either the



tumbling distribution assumed in the original model, or the number of tumbles per step (i.e. prior to communicating a new location). While the former (a uniform tumbling distribution) is less likely in practice, the latter (communicating only when a new descent direction is established) both makes biological sense [21] and, as we show empirically in Results, reduces the time it takes the swarm to reach the food source. For the second lemma we again need to modify the original algorithm so that the step size (amount of progress made in the direction computed) is proportional to the detected gradient, causing the agents to slow as they approach the food source. This may be implemented in practice via a feedback loop used by bacterial cells [22]. Detailed assumptions and rigorous proofs of both lemmas and the convergence theorem are given in the Supplement.

## **Empirical Results**

To determine whether the restricted communication model we assume can indeed lead to efficient convergence we performed several simulations of bacterial food search. First, we compare the search efficiency of bacterial food search with and without communication, and between our model and the Shklarsh et al. model. Second, we introduce multiple swarms and test how their trajectories affect each other. Third, we explore the predictions of the model for a setting in which a fraction of the bacteria are behaving differently than the others. This latter point is of great current interest since ‘cheaters’ (cells that receive messages but do not spend the energy on sending them) may be responsible for a form of antibiotic resistance that has been recently observed [23]. Finally, we evaluate our method using new experimental data. Thus, the results presented below are of interest to both the computational part of this work (efficient and robust DGD model) and the biological aspects (models of bacterial coordination).

To save space, in the remainder of this section we refer to the Shklarsh et al. model as the ‘DE’ model and our model as the ‘DGD’ model (even though both rely on updating magnitude and direction in time steps).

## Performance on a realistic food search simulation

To evaluate the performance of our method we first tested it using the terrain and obstacle model from Shklarsh et al. [12] (see Supplement). In these settings we varied the number of agents, the communication between agents and the number of swarms.

The quantity we compared was the time it took cells to reach the food source (in terms of steps, since both algorithms can be run synchronously). Figure 2 presents the distribution of the number of steps it takes cells to reach the food source under several different models.

The first is a model without communication (i.e. each cell can only sense the food gradient, but does not receive or send any message). The second is the Shklarsh et al. model with adaptive weighting, and the other two models are our DGD model with fixed or variable step size (the latter is required for the convergence proof above while the former is usually used in bacterial models). As can be seen, communication greatly improves the time it takes cells to reach the food source, which may explain why such a secretion-based communication system has evolved in this species. As for the specific communication model, the DGD model improves the results when compared to the DE model, even though our DGD model severely restricts the set of messages that can be used. In fact, the discretization of messages decreases both the mean and variance of the distribution. This is likely due to the fact that, by thresholding, the discretization step is effectively reducing the large noise that can be associated with individual messages. In addition, the distance-weighted edges (corresponding to the diffusion rates of secreted communication molecules) also improve the performance of the method. Simulation movies with and without communication between cells can be observed on the Supporting Website.

Figure 3 displays the effect on the time it takes cells to reach the food source if another swarm is added to the simulation. In this sequential set up, the second swarm starts 50 iterations after the first swarm. As can be seen, the fact that the first swarm was already able to successfully navigate to the food source enables the second swarm to utilize (at least partially) the trajectory they identified to further reduce the time it takes to reach the food. Interestingly, while the improvement for the second swarm is indeed large, we also see a *decrease* in the performance of the first swarm compared to the single swarm result presented in Figure 2. This is due to the negative influence that the second swarm has on the first when it enters the region of influence.

Since the second swarm starts in the opposite direction of the food source, the first swarm is (partially) adjusting its direction incorrectly (based on attraction to cells in the second swarm) increasing the number of iterations it takes cells to reach the food source.

### **Sensitivity to silent agents**

Previous work has shown that some cells in a population become ‘silent’ [25],[26], [27]. These cells receive messages from the other cells but do not send messages themselves. While such behavior is beneficial from the individual standpoint (less energy is required to synthesize and secrete the signaling molecules) it may be harmful for the population as a whole since if these ‘silent’ cells proliferate the population will lose its ability to utilize communication to improve food search. Recent work has shown that stochastic activation of such silencing and other individual behavior mechanisms can explain how they can be advantageously used (for example, for developing antibiotics resistance) without affecting the overall ability of cellular coordination. We have thus used the obstacle model again to study the sensitivity of swarm performance to the fraction of silent cells in the population. For this, we varied the fraction of silent agents from 0 to 1. As can be seen in Figure 4 up to a certain threshold we do not see a large impact for the increase in silent cells which supports the recent findings of [23]. Specifically, based on our models the performance of the population is only 20% less than optimal even if 85% of the cells are silent.

We have further analyzed various aspects of the communication model to determine the roles of each type of message being sent (orientation, attraction) or sensed (physical proximity), in terms of the impact on the time taken to reach the food source. See Supplement for details.

### **New experimental data: Chemotactic migration of *E. coli* cells with or without cell-cell communication**

We designed and fabricated a microfluidic device to test aspects of our model. We studied the chemotactic migration behavior of wild type (wt) and  $\Delta tsr$  mutant *E. coli* cells in the microchambers in the presence of chemoattractant gradient. While the initial modeling assumed a swarm of agents at the start, due to the technical constraints, in our experiments the cells were evenly distributed in the microchambers at the beginning. After the media with chemoattractant was introduced in the main channel, gradients of the chemoattractant were generated in the

microchambers, with high concentration of the chemoattractant at the inlet corner and lower concentration at the other three corners (Figure 5). As seen in the supplementary movies and Figure 5b), the *E. coli* cells in the microchambers sense the gradient and migrate toward the inlet corner before escaping into the main channel. Previous studies [28] confirmed that motility buffer and the deletion of the Tsr chemoreceptor would not decrease the motility and chemotactic migration speed of *E. coli* cells to Aspartic acid (which engages the Tar chemoreceptor). However, cells in the nutrient-deprived motility buffer cannot secrete the amino acid glycine while cells lacking the Tsr receptor cannot sense the gradient of glycine. It has been previously shown that glycine plays a key role for several collective behaviors of starved *E. coli* cells. In a nutrient-depleted environment, the *E. coli* RP437 cells can sense and be attracted by glycine secreted by other cells forming dense aggregates [28]. Indeed, in our experiments, WT *E. coli* cells in M9CG medium migrate much faster than wt cells in motility buffer and  $\Delta tsr$  mutant cells in M9CG. More than 90% of wt cells escaped from the microchamber in 10 minutes in M9CG, while only 60% cells escaped after 60 minute exposure to the chemoattractant gradient in the two control experiments (Figure S6). As the cells in the two control experiments can neither secrete glycine (in motility buffer) nor sense glycine ( $\Delta tsr$  cells) no cell-cell communication is expected and observed in these experiments. This result agrees with our model assumptions about the importance of cell to cell communication in bacterial food search.

### Comparing model based simulations with experimental data

To further test the DGD model and compare it with the Shklarash DE model, we used both models to simulate bacterial food search with the same initial configuration as the experimental setting (initially cells are evenly distributed rather than grouped in a swarm). We next performed analysis to determine the ratio of the number of cells at the food source (bottom right corner) to the number of cells at the opposite corner for each minute / iteration in the experiment and simulations, respectively (Methods). This process was repeated for the three different obstacle sets we tested (these varied in their sizes for each experiment but the overall coverage remained the same for all obstacle sizes (Methods)). The results, comparing the two models and the experiments are presented in Figure 5 (each simulation curve is averaged over 50 random starts). As can be

seen, and as expected, both models and experiments agreed that the ratio increases as time / iteration increase due to cell attraction to the food source. The models also correctly agreed on the ordering of the different obstacle sizes in terms of the ratio (recall that the coverage is the same, and so bigger obstacles also mean fewer overall obstacles allowing for easier navigation if communication is allowed). However, the models differed in the slope of the predicted ratio increase and in the similarity between the different obstacle sizes. Overall, we observe that the DGD model leads to slopes that are in better agreement with the experimental results. In addition, in the DGD model the two larger obstacle setups are grouped together and are separated from the smallest whereas in the DE model the two smaller settings are grouped together and separated from the largest. Here again the experimental results correlate more closely with the DGD model.

## Discussion and conclusions

We have shown, both theoretically and in simulations and experiments, that a distributed gradient descent model can efficiently interpret the communication of agents under severe limitations. These include limits on the complexity of messages and the ability to identify which agent is sending the message, while at the same time assuming a dynamic environment where neighbors' locations (and their influence) change constantly. We have proved that, under reasonable biological assumptions, the communication algorithm discussed is likely to converge, helping to explain how bacteria can efficiently coordinate food search in harsh environments and improving upon prior models of this process. Moreover, the social dynamics of bacteria can also affect their ability to resist antimicrobial therapy, and inhibition of bacterial cooperation is an alternative approach to minimize collective resistance [29].

Our convergence proof only holds for the attraction information and does not hold for the repulsion and direction components of the computation performed by each agent. Since the orientation information is also a vector averaged over all neighbors, we believe that the proof can be extended to include this communication term as well, though a key challenge would be to understand the sometimes competing goals of local versus global improvement near certain obstacles. Repulsion is more difficult to analyze because it is not based on averages. However, as we show in the Supplement, the attraction term has by far the most significant effect on swarm performance

while the other two communication terms have a much less significant impact on the time it takes cells to reach the food source. Hence, for computational applications of our method, it may suffice to use the attraction term, in which case convergence is guaranteed.

## Methods

### Bacterial strains and growth conditions

The wild-type *E. coli* RP437 strain and its derivative HCB317 ( $\Delta tsr$ , from the lab of Prof. Howard Berg), were used throughout the study. Cultures were launched from a frozen stock and grown overnight at  $30^{\circ}C$  with agitation at  $240rpm$  in M9 minimal medium supplemented with  $1g/l$  casamino acids and  $4g/l$  glucose (M9CG). We then diluted the overnight culture hundredfold in the morning with fresh M9CG and the cells were harvested at early log phase ( $OD_{600nm} = 0.1$ ). Prior to experiments we centrifuged, washed and resuspended the cells in M9CG or motility buffer (10 mM potassium phosphate, 10 mM sodium lactate, 0.1 mM EDTA, and 1 mM L-methionine,  $pH=7.0$ ). We added chloramphenicol ( $30\mu g/ml$ ) to all media to maintain the plasmid expressing yellow fluorescent protein (YFP) or red fluorescent protein (tdTomato) constitutively in the cells.

### Preparation of microfluidic device

We designed a microfluidic device that contain three different designs of evenly distributed micropillars (obstacles) within  $1000 \times 1000\mu m^2$  microchambers that in their totality occupy 25% of the total surface area (Figure 5 a)). All chambers are connected to a wide channel through a  $5\mu m$  wide channel to allow for the introduction of cells and media. The layout of the device is shown in Figure 5a).

We fabricated the microdevice using standard soft lithography. Briefly,  $10\mu m$ -thick photoresist SU-8 2010 (MicroChem, Newton, MA) was spin-coated onto a polished silicon wafer. The spin-coated wafer was then exposed to UV light through the photomask by Karl Suss MJB3 aligner. Unexposed resist was removed with a SU-8 developer so that a raised surface remained that was the negative of the desired structure. The microfluidic device was cast from the biologically inert polymer PDMS (Sylgard 184, Dow Corning), which was heat-cured on the mold at  $65^{\circ}C$  and then peeled away. After inlet-outlet holes were cut, the PDMS chips were briefly treated in air plasma cleaner for 30 seconds to render them hydrophilic and to enable the PDMS to seal to a thin glass coverslip. Immediately after the plasma treatment and bonding,  $5\mu L$  of  $20mg/mL$  BSA solution was added into the two holes in the PDMS. Both holes were then sealed with masking tape. The device was kept at room temperature for at least one hour to coat the PDMS channel walls with

a thin layer of BSA. The BSA solution in the microchannels and microchambers was replaced with M9CG or motility buffer after surface passivation.

The motile cells which were resuspended in M9CG or motility buffer were then introduced into the main channel and was allowed to swim continuously into the microchambers. After reaching the desired cell density in the microchambers, fresh M9CG or motility buffer containing  $300\mu M$  L-aspartic acid (MP Biomedicals) as chemoattractant was pumped into the main channel at a flow rate of  $5\mu L/min$ .

### **Time-lapse imaging and data analysis**

The chemotactic response of the fluorescently labeled *E. coli* cells was observed and recorded on a fully automated inverted microscope (Zeiss AxioObserver Z1) equipped with a motorized stage (Applied Scientific Instruments) and an external LED light source (Metaphaser MP-LE1007) for fluorescence. The time-lapse movies were collected every minute with a CCD camera (Zeiss Axio-Cam MRm) at room temperature ( $\sim 27^\circ C$ ). The movies were processed for display with ImageJ software. The cell number in the microchambers at each image frame was counted automatically by a custom pipeline with the open-source software Cellprofiler.

### **Analysis of movies to identify concentration at food source**

We quantified the time it takes cells to reach the food source by tracking the ratio of the cell concentration at the bottom right corner (chemoattractant inlet) and top left corner (lowest concentration of chemoattractant) of the chamber (Figures 5a) and b). For each corner we considered a quarter circular area of fixed radius (200 pixels) to measure cell concentration. In the biological experiments, after reaching the food source cells escape through the inlet. Therefore the total number of cells in the chamber decreased with time. To allow for comparison with the simulation results in which the total number of cells in the chamber is fixed we normalized the ratio of cell concentrations in the experiments by total cell count at each time point.



## References

1. Seeley T. D. (2002). When is self-organization used in biological systems?. *Biol. Bull.*, 202(3),314-318.
2. Babaoglu O. et al (2006). Design Patterns from Biology for Distributed Computing. *ACM Transactions on Autonomous and Adaptive Systems*, 1:26-66.
3. Cheong, R., Rhee, A., Wang, C. J., Nemenman, I., Levchenko, A. (2011). Information transduction capacity of noisy biochemical signaling networks. *Science*, 334(6054),354-358.
4. Ong, K. G. et al. (2004). A wireless sensor network for long-term monitoring of aquatic environments: Design and implementation. *Sensor Letters*, 2(1), 48-57.
5. Navlakha, S., Bar-Joseph, Z. (2014). Distributed information processing in biological and computational systems. *Communications of the ACM*, 58(1), 94-102.
6. Hopfield, J. J. (1982). Neural networks and physical systems with emergent collective computational abilities. *Proc. of the Nat. Academy of Sciences*, 79(8), 2554-2558.
7. Bishop, C. M. (1996). *Neural Networks for Pattern Recognition*, 1st edn. USA: *Oxford University Press*
8. Hastie, T., Tibshirani, R., Friedman, J., Hastie, T., Friedman, J., Tibshirani, R. (2009). *The elements of statistical learning*, 2(1). New York: springer.
9. Mezard, M., Montanari, A. (2009). *Information, physics, and computation*. Oxford University Press.
10. Waters, C. M., Bassler, B. L. (2005). Quorum sensing: cell-to-cell communication in bacteria. *Annu. Rev. Cell Dev. Biol.*, 21, 319-346.
11. Torney, C., Neufeld, Z., Couzin, I. D. (2009). Context-dependent interaction leads to emergent search behavior in social aggregates. *Proc. of the Nat. Academy of Sciences*, 106(52), 22055-60.
12. Shklarsh, A., Ariel, G., Schneidman, E., Ben-Jacob, E. (2011). Smart swarms of bacteria-inspired agents with performance adaptable interactions. *PLoS comp. bio.*, 7(9), e1002177.
13. Tsitsiklis, J. N., Bertsekas, D. P., Athans, M. (1986). Distributed asynchronous deterministic and stochastic gradient optimization algorithms. *IEEE trans. on auto. control*, 31(9), 803-812.
14. Anastasi, G., Conti, M., Di Francesco, M., and Passarella, A. (2009). Energy conservation in wireless sensor networks: A survey. *Ad hoc networks*, 7(3), 537-568.
15. Zinkevich, M., Weimer, M., Li, L., and Smola, A. J. (2010). Parallelized stochastic gradient descent. In *Advances in neural information processing systems* (pp. 2595-2603).
16. Li, F., Wu, B., Xu, L., Shi, C., and Shi, J. (2014). A fast distributed stochastic gradient descent algorithm for matrix factorization. In *Proceedings of the 3rd International Workshop on Big Data, Streams and Heterogeneous Source Mining: Algorithms, Systems, Programming Models and Applications* (pp. 77-87).
17. Koutra, D., Ke, T. Y., Kang, U., Chau, D. H. P., Pao, H. K. K., Faloutsos, C. (2011). Unifying guilt-by-association approaches: Theorems and fast algorithms. In *Machine Learning and Knowledge Discovery in Databases*, 245-260. Springer Berlin Heidelberg.
18. Rubenstein, M., Cornejo, A., Nagpal, R. (2014). Programmable self-assembly in a thousand-robot swarm. *Science*, 345(6198), 795-799.
19. Wartlick, O., Kicheva, A., Gonzalez-Gaitn, M. (2009). Morphogen gradient formation. *Cold Spring Harbor perspectives in biology*, 1(3), a001255.
20. Emek, Y., Wattenhofer, R. (2013, July). Stone age distributed computing. In *Proc. of the 2013 ACM symp. on Principles of distributed computing*, 137-146.
21. Hense, B. A., Kuttler, C., Mller, J., Rothballer, M., Hartmann, A., Kreft, J. U. (2007). Does efficiency sensing unify diffusion and quorum sensing?. *Nature Rev. Microbiology*, 5(3), 230-239.
22. Vladimirov, N., Løvdok, L., Lebedz, D., Sourjik, V. (2008). Dependence of bacterial chemotaxis on gradient shape and adaptation rate. *PLoS computational biology*, 4(12), e1000242.
23. Yurtsev, E. A. et al (2013). Bacterial cheating drives the population dynamics of cooperative antibiotic resistance plasmids. *Molecular systems biology*, 9(1).
24. Taylor, Rion G., and Roy D. Welch. 'Chemotaxis as an emergent property of a swarm.' *Journal of bacteriology* 190.20 (2008): 6811-6816.
25. Velicer, G. J., Kroos, L., Lenski, R. E. (2000). Developmental cheating in the social bacterium *Myxococcus xanthus*. *Nature*, 404(6778), 598-601.
26. Hammerschmidt, K., Rose, C. J., Kerr, B., Rainey, P. B. (2014). Life cycles, fitness decoupling and the evolution of multicellularity. *Nature*, 515(7525), 75-79.
27. Strassmann, J. E., Zhu, Y., Queller, D. C. (2000). Altruism and social cheating in the social amoeba *Dictyostelium discoideum*. *Nature*, 408(6815), 965-967.
28. Park, Sungsu, et al. (2003). Influence of topology on bacterial social interaction. *Proceedings of the National Academy of Sciences* 100.24: 13910-13915.
29. Vega, N. M. and Gore, J. (2014) Collective antibiotic resistance: mechanisms and implications. *Curr Op. Microbiol* 21, 28-34.

**Figure 1 Environment and model assumptions**

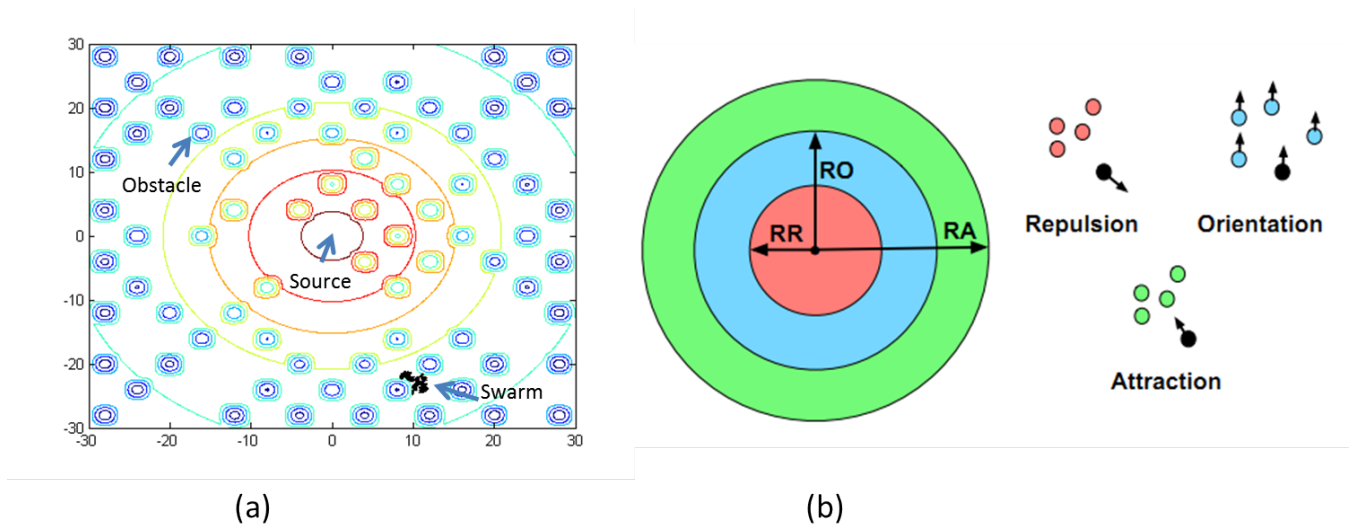


**Fig. 1. (a):** Terrain model for bacterial food search. Obstacles are randomly placed and the food source is at the center of the region. Contours display the diffusion of the food source gradient. **(b):** Dynamics of repulsion, orientation, and attraction for a single bacterial cell in the Shklarsh et al. model.  $RR$  = radius of repulsion,  $RO$  = radius of orientation, and  $RA$  = radius of attraction. While we still maintain the physical ( $RR$ ) versus communication ( $RO$ ,  $RA$ ) split between the repulsion and attraction / orientation information, our model does not assume that the identity of the sender is known and so it does not distinguish cells in the  $RO$  and  $RA$  locations.

Figure 2: Comparison of search time under different communication models

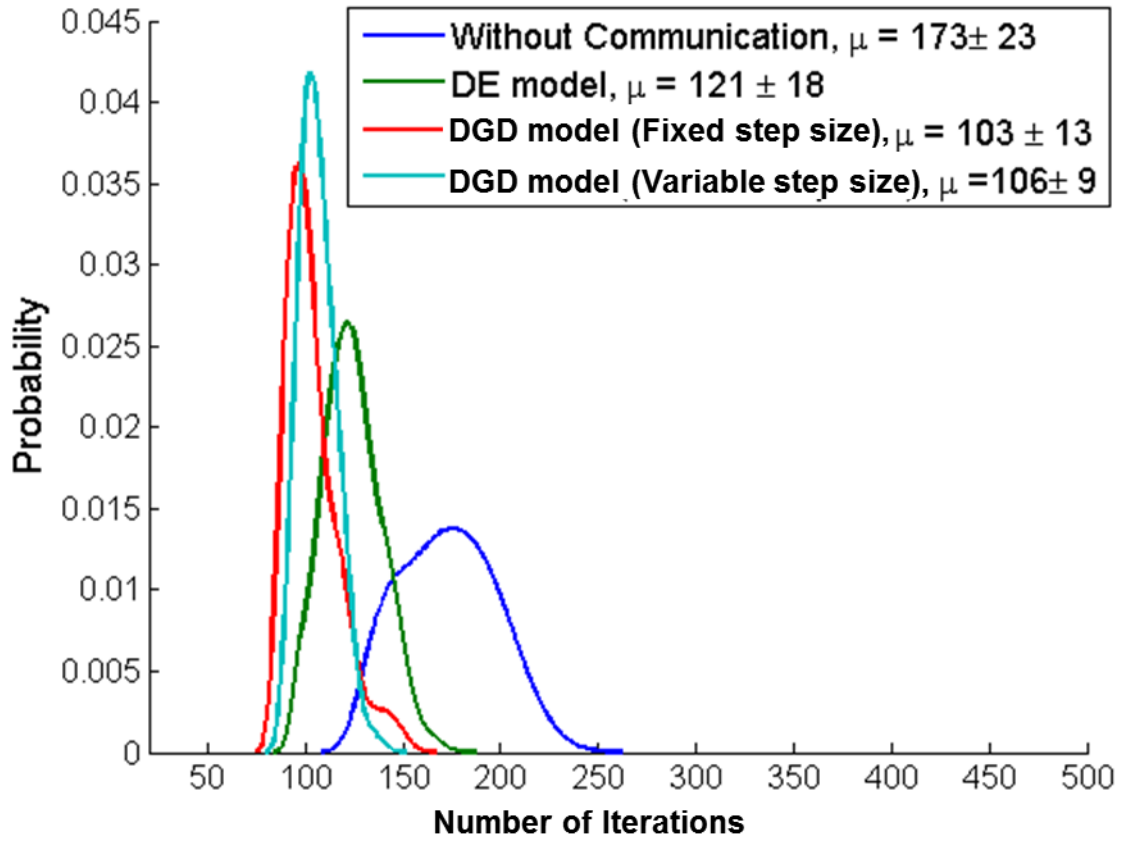
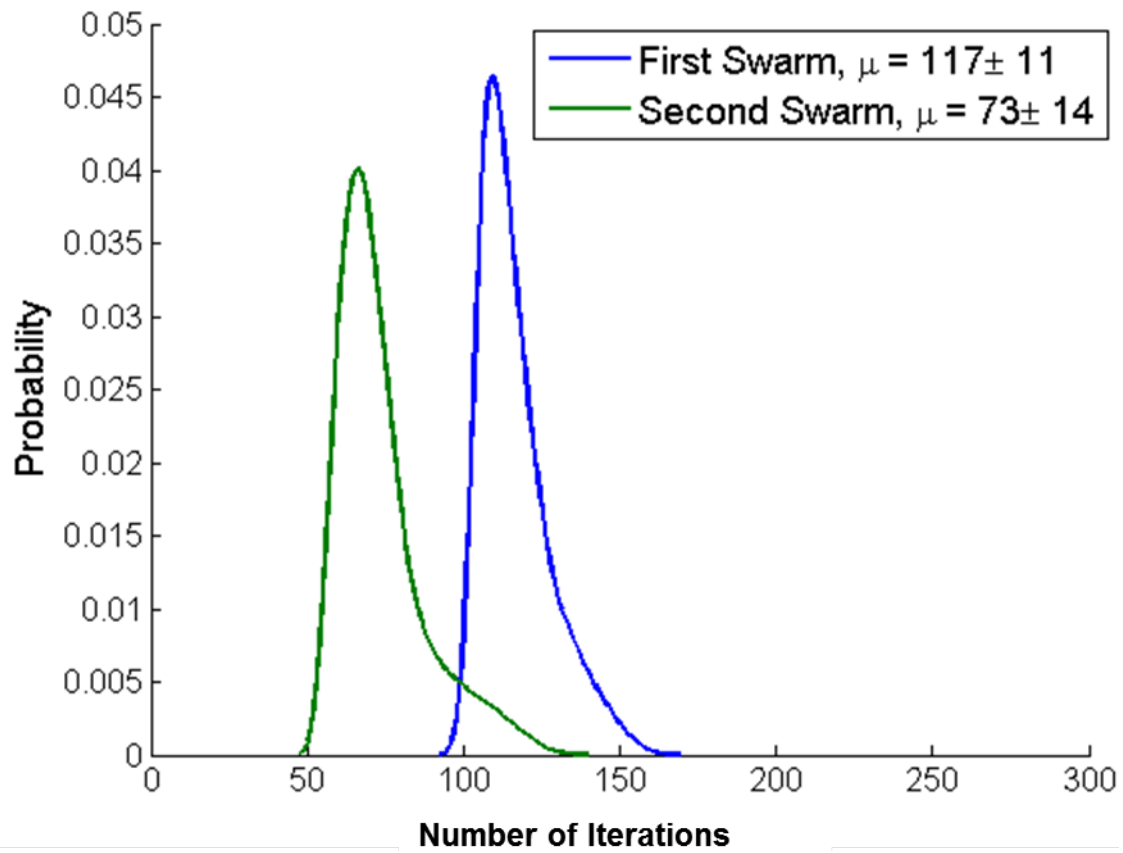


Fig. 2. Comparison between the original Shklarsh model and the DGD model.  $\mu$  denotes the mean number of iterations per agent, plus or minus the standard deviation.

Figure 3: Performance of multiple swarms



**Fig. 3.** Distribution of number of iterations for two sequential swarms using variable step sizes.  $\mu$  denotes the mean number of iterations per agent.

Figure 4: The effects of silent agents

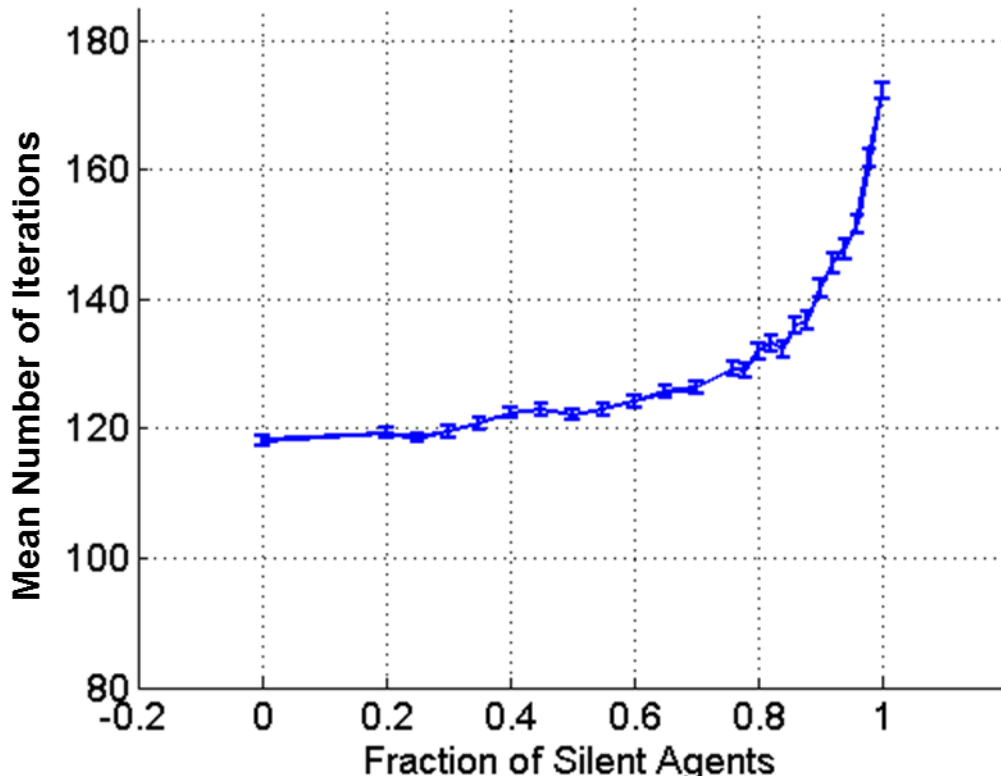
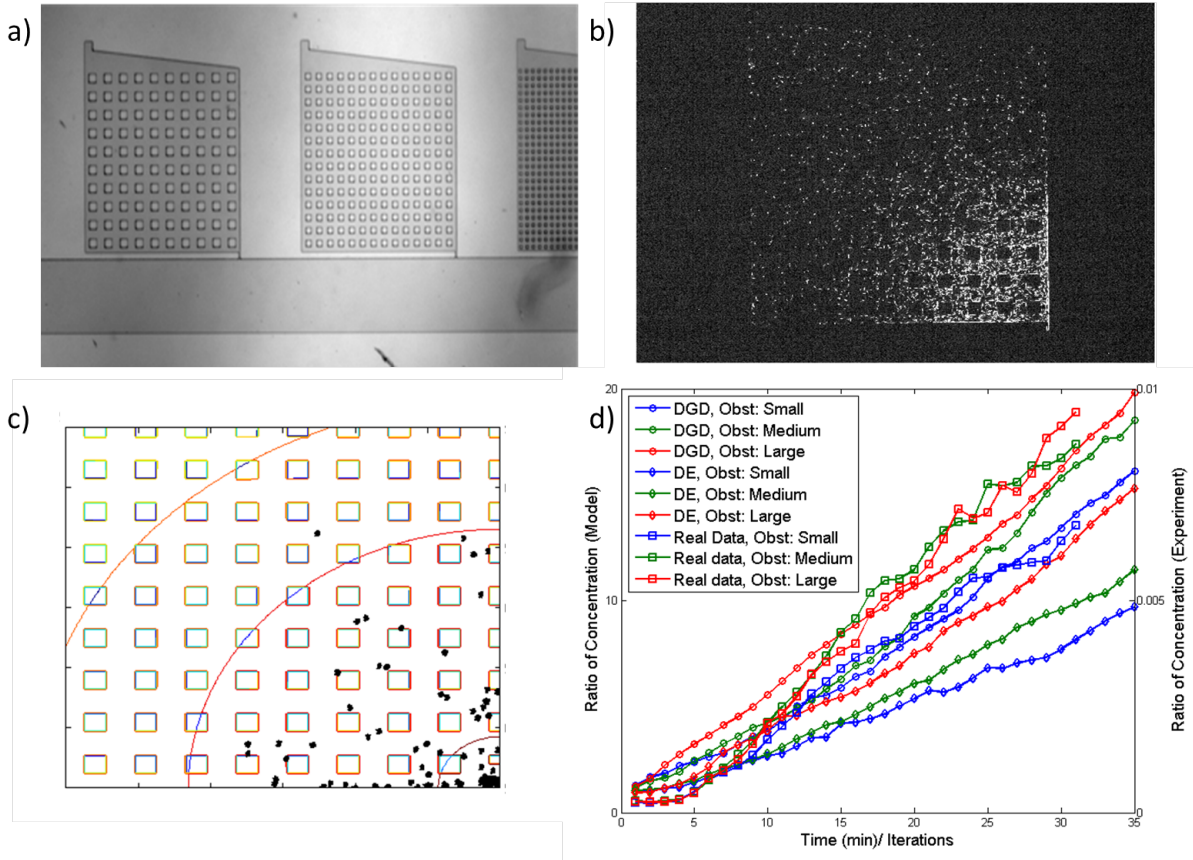


Fig. 4. Mean path lengths over silent fractions, based on 100 trials. More silent bins were taken in the range of .7 to 1 to illustrate the phase transition. Error bars indicate standard deviations.

**Figure 5: Experimental results**



**Fig. 5.** Experimental validation of the model a) Experimental setup. Microchambers with three different obstacle patterns though with the same overall coverage, b) Snapshot of chemotaxis movie, showing higher concentration of cells at the food source inlet (bottom right). Obstacles can be observed as dark rectangles surrounded by white cells. , c) Simulation setup mimicking experiment, d) Comparison of DGD and DE models with experimental data. As can be seen, the DGD simulation results lead to slopes and groupings that are in better agreement with the experimental results.

# Supplementary Information: Distributed Gradient Descent in Bacterial Food Search

Shashank Singh<sup>\*1</sup>, Sabrina Rashid<sup>\*2</sup>, Zhicheng Long<sup>3</sup>, Saket Navlakha<sup>4</sup>, Hanna Salman<sup>5</sup>, Zoltán N. Oltvai<sup>6</sup>, Ziv Bar-Joseph<sup>7†</sup>

<sup>1</sup> Machine Learning Department and Department of Statistics, Carnegie Mellon University, Pittsburgh, PA 15213.

<sup>2</sup> Computational Biology Department, Carnegie Mellon University, Pittsburgh, PA 15213.

<sup>3</sup> Department of Pathology, Department of Physics and Astronomy, University of Pittsburgh, Pittsburgh, PA 15213.

<sup>4</sup> The Salk Institute for Biological Studies, Center for Integrative Biology, La Jolla, CA 92037.

<sup>5</sup> Department of Physics and Astronomy, Department of Computational and Systems Biology, University of Pittsburgh, Pittsburgh, PA 15260.

<sup>6</sup> Department of Pathology, Department of Computational and Systems Biology, University of Pittsburgh, Pittsburgh, PA 15260.

<sup>7</sup> Machine Learning Department and Computational Biology Department, Carnegie Mellon University, Pittsburgh, PA 15213.

\* These authors contributed equally.

† Contact author. Email: zivbj@cs.cmu.edu

## Supporting Methods

### Complete update rule for a single cell

Below we present the complete update rule performed by each cell in each of the steps of the algorithm to compute its new trajectory. At each iteration, there are three communication components in the BP model, i) repulsion, ii) orientation, and iii) attraction.

As discussed in the main text, we divide the update into two cases. If there are *any* cells within the Repulsion Radius (RR, determined by physical interactions) then the cell moves as follows:

$$\mathbf{u}_i(n) = - \sum_{j \in B_{RR}} \frac{\mathbf{x}_i(n) - \mathbf{x}_j(n)}{\|\mathbf{x}_i(n) - \mathbf{x}_j(n)\|}, \quad (1)$$

where  $x_i(n)$  is the location of agent  $i$  at time  $n$ . Otherwise (if there are no cells in RR) we set:

$$\mathbf{u}_i(n) = D_{L,T} \left( \sum_j \exp(-C_o \|\mathbf{x}_i(n) - \mathbf{x}_j(n)\|) \mathbf{v}_j(n) + \sum_j \frac{\exp(-C_a \|\mathbf{x}_i(n) - \mathbf{x}_j(n)\|) (\mathbf{x}_i(n) - \mathbf{x}_j(n))}{\|\mathbf{x}_i(n) - \mathbf{x}_j(n)\|} \right). \quad (2)$$

In either case, the cell updates its own position by moving according to

$$x_i(n+1) = x_i(n) + \gamma_i(n)(u_i(n) + s^i(n)),$$

where  $s^i(n)$  is the belief of cell  $i$  at time  $n$  based on its sensing of the food gradient ( $s^i(n)$  is a pseudogradient, as shown in Lemma 1 below).  $\gamma_i(n)$  is the step size for agent  $i$  at time  $n$ , which, as discussed in the main text, is a function of the food gradient at the cell's location (a detailed formulation of  $\gamma_i(n)$  is in the proof of Lemma 2 below).

## Convergence Theorem

In a simplified model that incorporates only the attraction term of communication, our convergence theorem follows from a general convergence theorem proven by Tsitsiklis et al. for a broad class of distributed pseudogradient descent algorithms (Theorem 3.1 and Corollary 3.1 of [1]). Work is needed only to show that our setting satisfies the six assumptions therein (listed and justified below). In order to match the notation of [1], we note that the update equation (using only the attraction term) can be written in the form

$$x_i(n+1) = \sum_j^M a_{ij}(n)x_j(n) + \gamma_i(n)s^i(n) \quad (3)$$

where  $a_{ij}(n)$  is the edge weight between cells  $i$  and  $j$  at time  $n$ .

**Convergence Theorem:** Let  $x_i(n) \in \mathbb{R}^2$  denote the position of the  $i^{\text{th}}$  agent at time  $n$  and let  $J : \mathbb{R}^2 \rightarrow \mathbb{R}$  denotes the concentration of the food source (the objective function). Under assumptions A1-A6 (see below), the following hold:

1. There exists a constant  $\gamma^* > 0$  such that, if each step size is at most  $\gamma^*$  (i.e.,  $\sup_{i,n} \gamma_i(n) \leq \gamma^*$ ), then, with probability 1, for all distinct agents  $i$  and  $j$ ,

$$\lim_{n \rightarrow \infty} (x_i(n) - x_j(n)) = 0.$$

2. If, in addition, the level sets of  $J$  are compact, then, with probability 1, for all agents  $i$ ,

$$\lim_{n \rightarrow \infty} \|\nabla_x J(x_i(n))\|_2 = 0.$$

3. Finally, if, in addition, all stationary points of  $J$  are minima (e.g., if  $J$  is convex), then, with probability 1, for all agents  $i$ ,

$$\lim_{n \rightarrow \infty} J(x_i(n)) = \inf_x J(x).$$

The three components of the above theorem gives sufficient conditions for the agents to converge spatially, to converge to a connected set of stationary points, and to converge to a connected set of minima, respectively. Assumptions A1-A4 (stated precisely below) are that  $J$  is sufficiently smooth (its gradient is Lipschitz continuous) and that the agents' communication network is sufficiently dense so that information from any agent eventually propagates through the swarm. Assumptions A5 and A6 correspond to Lemmas 1 and 2 which we explicitly discuss below.

The lemmas, stated below, are needed to establish that our algorithm is indeed a distributed pseudogradient algorithm before we can apply the results of [1]. The lemmas essentially state that (a) the agents expect to move in a descent direction and (b) the variance in the agent's movements is at most proportional to the magnitude of the true gradient (so that, for example, it vanishes near stationary points and hence agents cease to explore once they have located an optima).

**Assumptions** The assumptions needed for the general convergence proof are the following:

- A1** There is some  $\alpha > 0$  such that  $a_{ij}(n) \geq \alpha$ , for all times  $n$  and distinct agents  $i$  and  $j$ .  
**A2** There exists a constant  $B$  such that the time between consecutive communications between any pair of distinct agents  $i$  and  $j$  is at most  $B_1$  [4],[5].



- A3** The number of messages communications between any two distinct agents during any duration of length  $B_1$  is bounded by some constant  $B_2$ .
- A4**  $J$  is continuously differentiable and its gradient  $\nabla_x J$  is Lipschitz continuous.
- A5** The conclusion of Lemma 1.
- A6** The conclusion of Lemma 2.

Below we discuss why each of these holds in our setting.

**A1** Since the edge weight  $a_{ij}(n)$  is a positive, strictly decreasing function of the distance  $\|x_i(n) - x_j(n)\|_2$  and the agents move only within a bounded region of  $\mathbb{R}^2$ , such an  $\alpha = \inf_{i \neq j, n} a_{ij}(n) > 0$  exists with high probability.

**A2, A3** This point is somewhat subtle, and quite important for the generality of our work. In our model, each agent regularly (after a fixed number of rounds on individual movement, as discussed in the proof of Lemma 1 below) measures the *weighted average* of the signals from all other agents in the swarm, through the update equation (3). The key observation here is that, in [1] (which only considers communication as being between pairs of agents, and hence phrases the assumption as above), each agent's update depends *only on the weighted average* of the messages received. Thus, this assumption is *weaker than* the assumption that the weighted average in the update equation incorporates *all* other agents (with weights satisfying the constraints of assumption A1). By construction, our model satisfies this.<sup>1</sup>

**A4** Food is assumed to diffuse smoothly from its source (usually according to a Bessel, Gaussian, or exponential decay function of distance).

**Lemma 1** Conditioned on the history of the algorithm, the expected gradient perceived directly by each agent (not accounting for information from the swarm) is a descent direction. That is,

$$E \left[ \frac{dJ}{dx}(x_i(n)) s^i(n) \right] \leq 0.$$

In order to guarantee this we will allow agents to tumble a fixed number of times between rounds of communication, so that, in expectation, they will find and move along a descent direction.

*Proof of Lemma 1:* We first show the case when the direction after a tumble is chosen uniformly at random, in which case, the proof is straightforward. For sake of generality, we then show the case where the new angle is chosen according to any distribution (such a Gaussian) satisfying a certain weak uniformity condition, allowing multiple tumbles within each round of communication.

*Uniform Case:* In each iteration  $n > 1$ , if the previous direction  $s^i(n-1)$  is not a descent direction (i.e., if  $J(x_i(n)) \leq J(x_i(n-1))$ ), then  $\frac{s^i(n)}{\|s^i(n)\|_2} \sim \text{Unif}(\partial B_1(0))$ ,<sup>2</sup> and the speed  $\|s^i(n)\|_2$  is deterministic given  $s^i(n-1)$  and  $x_i(n-1)$ . Since the function  $s \mapsto \nabla_x J(x_i(n)) \cdot s$  is linear, its expectation over a uniformly distributed variable is 0, and so

$$\mathbb{E} \left[ \nabla_x J(x_i(n)) \cdot s^i(n) \mid F_n \right] = \|s^i(n)\|_2 \mathbb{E} \left[ \nabla_x J(x_i(n)) \cdot \frac{s^i(n)}{\|s^i(n)\|_2} \mid F_n \right] = 0.$$

If the previous direction is a descent direction, the agent retains its previous direction.  $\square$

*General Case:* Now consider a more general algorithm parameterized by a *tumbling distribution* with density  $D$  on  $[-\pi, \pi]$  (above,  $D$  is uniform). In general, a single tumble may be

<sup>1</sup> Compare *Example V* of [1], which considers a similar communication pattern in a more abstract setting.

<sup>2</sup>  $B_1(0)$  denotes the unit ball centered at 0, and  $\partial B_1(0)$  denotes its boundary.

insufficient to ensure that the expected resulting direction is a descent direction, and so multiple tumbles may be necessary. We assume that  $D$  is somewhat uniform in the following sense:

$$0 < c := \inf_{\theta \in [-\pi, \pi]} \int_{\theta}^{\theta + \pi/2} D(\phi_{2\pi}) d\phi, \quad ^3$$

i.e., the agent has probability at least  $c \in (0, 1/4]$  of tumbling toward any particular quadrant. This assumption certainly holds for the Gaussian tumbling distribution we use in the main paper, but also allows a broad range of other possibilities, including any distribution whose density is lower bounded away from 0 on  $[-\pi, \pi]$ .

To prove the lemma, let  $\theta_0 = \theta(\nabla_x J(x_i(n)), s^i)$ ,  $\theta_{\ell+1} = \theta_{\ell} + \Delta\theta_{\ell}$ , where each  $\Delta\theta_{\ell} \sim D$  denotes the change in angle due to the  $\ell^{\text{th}}$  tumble. <sup>4</sup> With probability in  $(c, 1 - 3c)$ , any particular  $|\theta_{\ell}| \leq \frac{\pi}{4}$ , in which case

$$\nabla_x J(x_i(n)) \cdot s^i(n) \geq \frac{1}{\sqrt{2}} \|J(x_i(n))\|_2 \|s^i(n)\|_2.$$

Also, with probability in  $(2c, 1 - 2c)$ ,  $|\theta_{\ell}| \geq \frac{\pi}{2}$  for all  $\ell \in \{1, \dots, k\}$ , in which case, by the Cauchy-Schwarz inequality,  $\nabla_x J(x_i(n)) \cdot s^i(n) \geq -\|J(x_i(n))\|_2 \|s^i(n)\|_2$ . Otherwise,  $|\theta_{\ell}| \in (\frac{\pi}{4}, \frac{\pi}{2})$ , so  $\nabla_x J(x_i(n)) \cdot s^i(n) \geq 0$ .

Let  $L \in \{0, \dots, k\}$  denote the last  $\ell$  at which  $\theta_{\ell} > \frac{\pi}{2}$  (i.e., after which, the agent maintains its current direction for the remaining  $k - \ell$  tumbles). Since  $L = \ell$  if and only if  $|\theta_0, \dots, \theta_{\ell}| \geq \frac{\pi}{2}$

$$\begin{aligned} \mathbb{E} [\nabla_x J(x_i(n)) \cdot s^i(n) | F_n] &= \sum_{\ell=0}^k \mathbb{E} [\nabla_x J(x_i(n)) \cdot s^i(n) | F_n, L = \ell] \mathbb{P}[L = \ell] \\ &\geq \sum_{\ell=0}^k \|\nabla_x J(x_i(n))\|_2 \|s^i(n)\|_2 \left( \frac{1}{\sqrt{2}}(k - \ell) - \ell \right) 2^{\ell} c^{\ell+1} \\ &= \frac{c \|\nabla_x J(x_i(n))\|_2 \|s^i(n)\|_2}{\sqrt{2}} \left( \sum_{\ell=0}^k (2c)^{\ell} (k - (1 + \sqrt{2}) \ell) \right). \end{aligned}$$

It is easy to see that this quantity is positive for sufficiently large  $k$ , since, as  $k \rightarrow \infty$ ,  $\sum_{\ell=0}^k \ell (2c)^{\ell}$  converges while  $k \sum_{\ell=0}^k (2c)^{\ell}$  diverges (recalling  $c \in (0, 1/4)$ ).  $\square$

**Lemma 2** The variance of the updates goes to zero as the cost function goes to zero. That is, for some  $K_0 > 0$ ,

$$\mathbb{E} [\|s^i(n)\|^2] \leq -K_0 \mathbb{E} \left[ \frac{dJ}{dx}(x_i(n)) s^i(n) \right].$$

*Proof of Lemma 2:* We assume here that the food follows an isotropic Gaussian distribution centered at the origin. That is, for some  $\sigma > 0$ ,  $\forall x \in \mathbb{R}^2$ ,

$$J(x) = \frac{1}{\sqrt{2\pi\sigma^2}} \exp\left(-\frac{\|x\|_2^2}{2\sigma^2}\right).$$

Then, for all agents  $i$  and times  $n$ ,

$$\frac{dJ}{dx}(x_i(n)) = -\frac{1}{\sqrt{2\pi\sigma^2}} \exp\left(-\frac{\|x_i(n)\|_2^2}{2\sigma^2}\right) x_i(n)$$

<sup>3</sup> For  $x \in \mathbb{R}$ ,  $x_{\pi} = ((x + \pi) \bmod 2\pi) - \pi$  denotes the angle in  $[-\pi, \pi]$  equivalent to  $x$ .

<sup>4</sup> For two vectors  $u$  and  $v$ ,  $\theta(u, v) = \cos^{-1}\left(\frac{u \cdot v}{\|u\|_2 \|v\|_2}\right)$  denotes the (smallest) angle between  $u$  and  $v$ . For notational convenience, we measure angles as lying in  $[-\pi, \pi]$ , with 0 denoting the direction of  $\nabla_x J(x_i(n))$ .

Plugging in

$$x_i(n) = \sum_j a_{ij}(n)x_j(n) + \gamma_i(n)s^i(n)$$

gives

$$\frac{dJ}{dx}(x_i(n)) = -\frac{1}{\sqrt{2\pi\sigma^2}} \exp\left(-\frac{\|x_i(n)\|^2}{2\sigma^2}\right) \sum_j a_{ij}(n)x_j(n) - \frac{1}{\sqrt{2\pi\sigma}} \exp\left(-\frac{\|x_i(n)\|^2}{2\sigma^2}\right) \gamma_i(n)s^i(n)$$

Now the right-hand side of the lemma:

$$\begin{aligned} & -K_0 \mathbb{E} \left[ \frac{dJ}{dx}(x_i(n))s^i(n) \right] \\ &= K_0 \mathbb{E} \left[ \frac{1}{\sqrt{2\pi\sigma^2}} \exp\left(-\frac{\|x_i(n)\|^2}{2\sigma^2}\right) s^i(n) \sum_j a_{ij}(n)x_j(n) + \frac{1}{\sqrt{2\pi\sigma^2}} \exp\left(-\frac{\|x_i(n)\|^2}{2\sigma^2}\right) \gamma_i(n)s^i(n) \cdot s^i(n) \right] \\ &\geq K_0 \mathbb{E} \left[ \frac{1}{\sqrt{2\pi\sigma^2}} \exp\left(-\frac{\|x_i(n)\|^2}{2\sigma^2}\right) \gamma_i(n)\|s^i(n)\|^2 \right] \\ &= \mathbb{E} \left[ \exp\left(-\frac{\|x_i(n)\|^2}{2\sigma^2}\right) K' \gamma_i(n)\|s^i(n)\|^2 \right] \geq \mathbb{E} [\|s^i(n)\|^2] \end{aligned}$$

when the step size  $\gamma_i(n)$  satisfies  $K' \gamma_i(n) \geq \exp\left(\frac{\|x_i(n)\|^2}{2\sigma^2}\right)$ .  $\square$

### Terrain Modeling and Swarm Initialization

We use a similar terrain model to the one used in [2]. Food density and terrain are stationary over time. Food is assumed to be diffuse through the terrain, with a global maximum at the source. Specifically, we modeled the food density as an isotropic Gaussian function:

$$J(r) = \frac{K}{\sqrt{2\pi\sigma^2}} \exp\left(-\frac{r^2}{2\sigma^2}\right). \quad (4)$$

In addition, we introduce random obstacles in the form of local minima. In particular, we use the half cosine function to generate field of obstacles:

$$g(r) = \min(0, -4(\cos(\pi r/4) + 0.5)),$$

from which we randomly remove a small number of obstacles to increase trial-to-trial variability.

Each swarm is generated by choosing *swarm center* at a certain fixed distance from the food source, with the angle along this distance circle chosen uniformly at random. Agents are placed uniformly in a small square centered at the swarm center, with the constraint that no agent starts on an obstacle. See Figure S1 for an example of a single trial initialization.

### Simulation parameters

The results presented in the paper are produced with swarms consisting of 30 agents (unless otherwise stated). For the simulation we use a Repulsion Radius of 0.1 and for the [2] model we use 4.0 for Orientation Radius and 4.3 for the Attraction Radius. The discretized thresholding operator  $D_{L,T}$  in our model used  $L = 4$  and  $T = 3$  (see [3]).

All the probability distributions are generated from 300 independent trials. For each trial the number of iterations required for at least 75% of the agents to reach within a fixed radius of the food source was measured. We have set this source radius at 2.5. For modeling the food source we have used  $\sigma^2 = 1000$  and  $K = 200$  in equation (4).

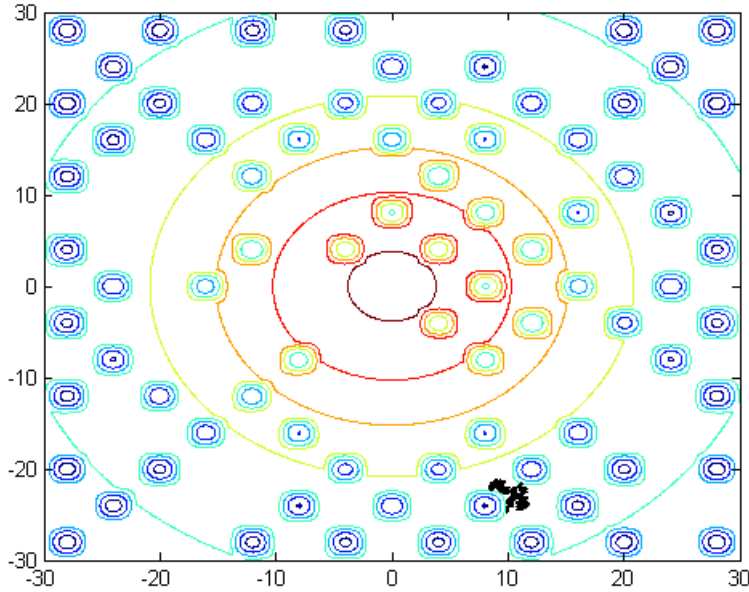


**Fig. S1.** A single swarm in our modelled terrain, immediately after initialization. Contour lines illustrate food concentration (maximized at the origin) and obstacles. Black dots indicate individual agents.

## Supporting Results

### Effect of different communication components

In addition to the results presented in the main paper we also tested the effects of each of the signals the agent / cell utilizes as part of the DGD model. These include: i) repulsion information, ii) orientation, and iii) attraction. We have evaluated the behavior of the swarms in the absence of either of these component to determine their impact of the ability of cells to efficiently reach the food source.

Figure S2 presents the simulation results for this analysis. As can be seen, while performance decreases when the orientation and repulsion components are disabled (average number of iterations required to reach the food source increases from 105 to 118 for repulsion and 105 to 115 for orientation) the effect is not large. In contrast the attraction component has a large effect on performance. Specifically, removing this component almost doubles the mean path length (168 iterations). One reason for this observation is that the decay in the weights of attraction components is one fourth of that of orientation (see methods section in the paper), providing opportunity for the swarms to have a longer range of interactions which dominates the swarm movement.

### Effect of using distances to weight messages

To test the impact of taking the distance into account when computing the local descent function we have run our method with and without using distance based weights, keeping all the other parameter settings same. Figure S3 presents the results of this analysis using two sequential

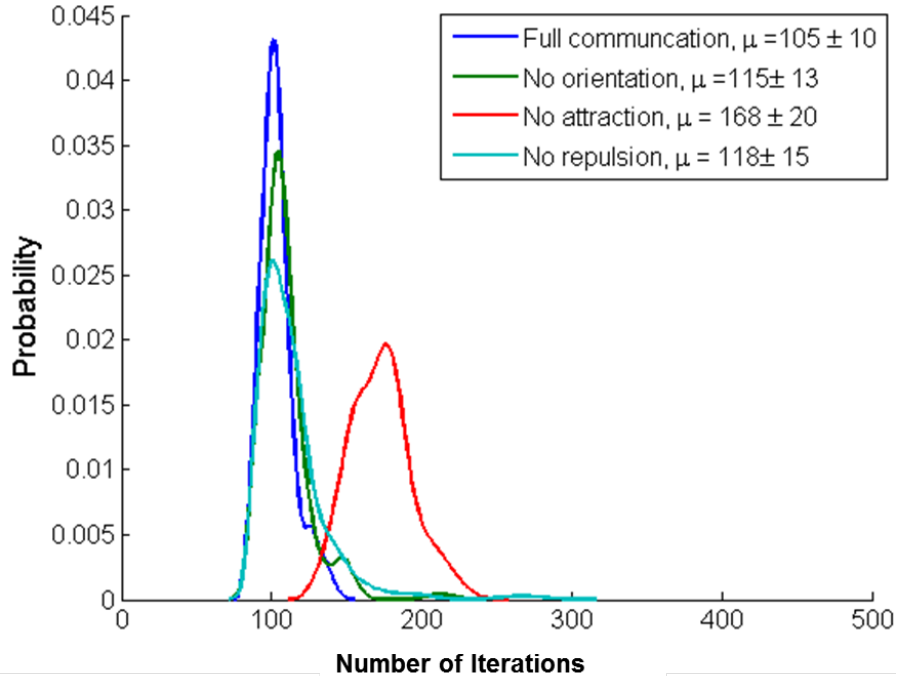


**Fig. S2.** Effect of the removal of different communication components.  $\mu$  denotes the average number of iterations required for each agent to reach the objective.

swarms. As can be seen, for both the first and second swarm, weighted communication leads to better performance than unweighted communication. Specifically, without using weights we see 10% and 22% increase in the number of iterations cells need to reach the food source for the first and second swarm, respectively. Thus, using the weighted version, which is also likely biologically correct, improves performance of such food search.

### Effect of swarm size

Another issue we tested is the impact of swarm size. As can be seen in Figure S4), overall performance improves with the increase in swarm size indicating that communication helps cells reach their goal faster. However, depending on how we model the repulsion distance, at some point such increase can lead to crowding. When the agents are too close to each other, their movement is highly constrained and mostly dominated by the repulsion effect. Therefore it takes much longer for a larger swarm to reach the food source. From our simulations we find that swarm size 30 to 50 gives the optimal performance.

### Model evaluation and comparison with previous experimental data

To further test our model and compare it with the Shklarsh et al. model we used experimental data from Taylor and Welch [6]. In their experiments, Taylor and Welch focus on the effects of mobility on swarm performance when a food gradient exists. Note that immobility of a large fraction of cells directly affects swarms coordination since those that are still mobile are receiving much fewer accurate messages impairing their ability to move in the correct direction. Thus, as the fraction of immobile cells increases, we expect several of the mobile cells to make at least

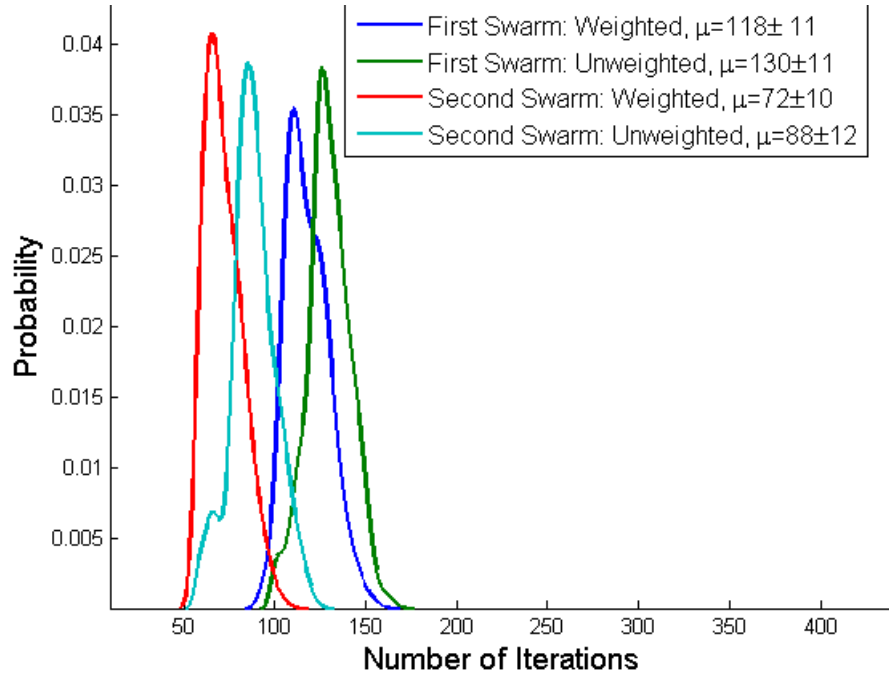


**Fig. S3.** Comparison of swarm performance using weighted and unweighted communication.  $\mu$  denotes the average number of iterations required for each agent to reach the objective.

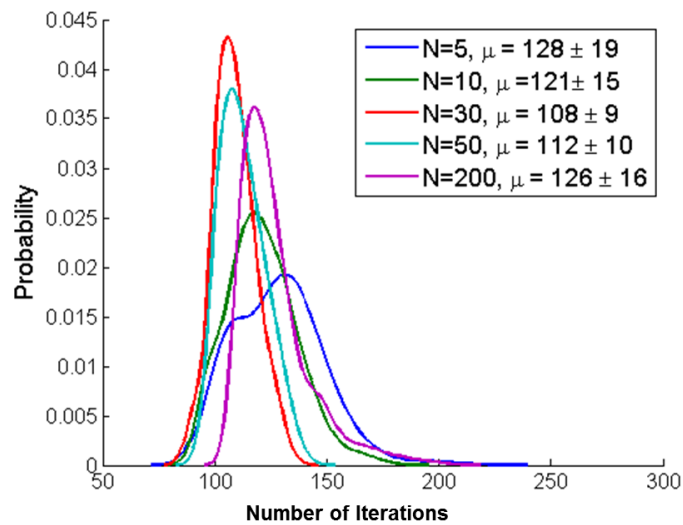


**Fig. S4.** Distribution of path length over different swarm sizes.  $N$  denotes the number of agents in the swarm and  $\mu$  denotes the average number of iterations required for each agent to reach the objective.

some moves in the wrong direction. Indeed, this is what Taylor and Welch observed in their experiments. To quantify the impact of immobile agents they measured the ratio between cells moving *towards* the food source and those moving *away* from the food source at a specific time point. Formally, we define this as:

$$TR_i = \frac{\max \left\{ d^S - d_i^j : d^S \geq d_i^j \right\}}{\left| \min \left\{ d^S - d_i^j : d^S \leq d_i^j \right\} \right|} \quad (5)$$

where  $TR_i$  denotes the tracking ratio during iteration  $i$ ,  $d^S$  is the initial distance of the swarm center from the food source and  $d_i^j$  is the distance of cell  $j$  from the food source at iteration  $i$ . In their experiments, cells start far enough from the food source such that the impact of the food gradient is minimal early on and so cells depend on swarm communication to move in the correct direction. Therefore, when a large fraction of cells is immobile the swarm would expand in both directions, leading to a TR that is close to 1. TR greater than 1 represents chemotactic (coordinated) movement.

When mobility is drastically impaired (only 1% of cells can move) Taylor and Welch report a TR of close to 1. The TR increases as the fraction of immobile cells decreases. These results were then used to identify mutants associated with movement since their TR was reduced when compared to WT cells.

To test our model in this setting we have simulated the immobilization of different fractions of cells and for each computed the resulting TR after a set number of iterations for each fraction. Figure S5 presents the resulting tracking ratios when using 10,000 cells. Note that while in our simulation we observe a TR that is higher than 1, even when only 0.5% are mobile, we attribute this to the far smaller number of cells in our simulations. For such a small set all mobile cells can likely communicate with all other mobile cells whereas when the number of cells is larger this ability may be reduced. However, as was observed in experimental results we also observe a rise in TR as the fraction of mobile cells increases. Further, while the TR obtained by our DGD method for the least constrained settings (3% mobile) is slightly higher than the TR for the same setting according to Shklarsh et al., the initial TR is significantly lower than the TR obtained by the Shklarsh model (and closer to the real result) indicating that our model can still capture the communication capabilities of bacterial cells with weaker assumptions and less computational power.

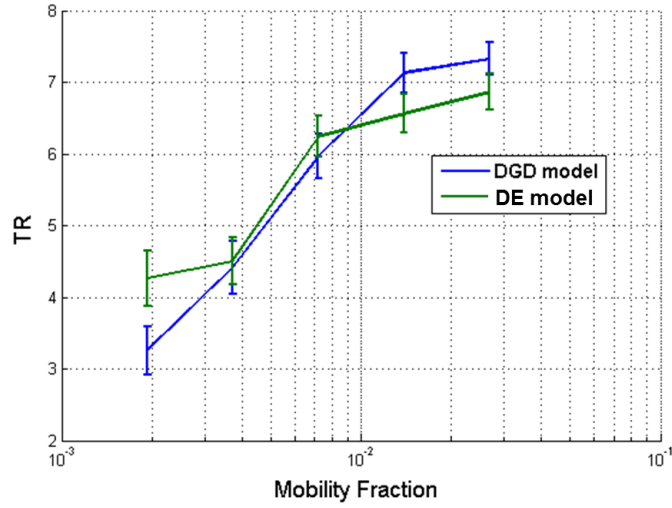


**Fig. S5.** Plot of TR vs mobility fraction. The results are generated with 300 independent trials using swarm population of 10000.

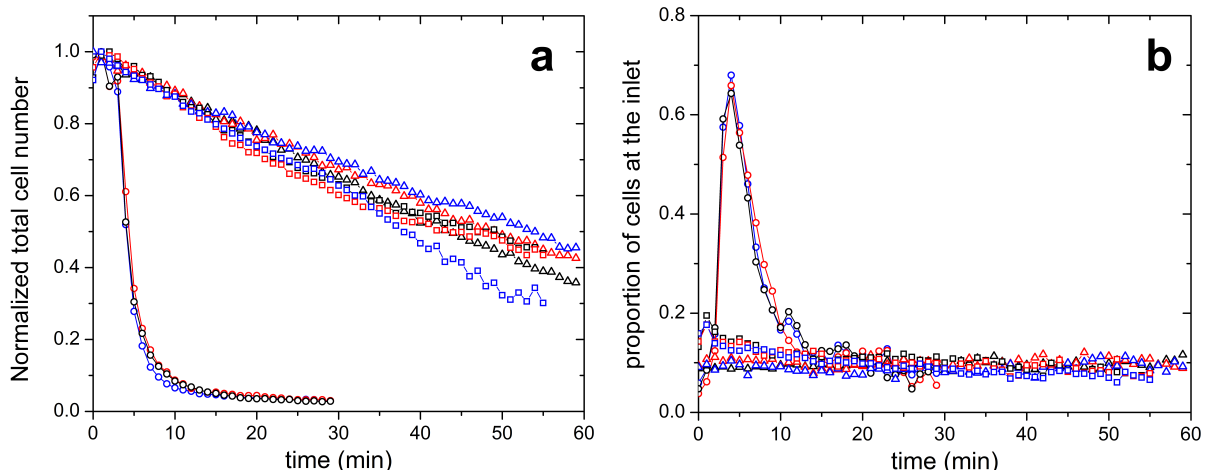


**Fig. S6.** The impact of communication on bacterial food search. Circles - WT bacteria. Rectangles - motility buffer, Triangles -  $\Delta tsr$ . (a) Total cell number in the whole chamber. (b) The proportion of cells in the inlet area (377 m radius from the inlet corner) as a function of time. Note that large increase in WT that is not observed in the communication-less conditions.



## References

1. Tsitsiklis, J. N., Bertsekas, D. P., Athans, M. (1986). Distributed asynchronous deterministic and stochastic gradient optimization algorithms. *IEEE trans. on auto. control*, 31(9), 803-812.
2. Shklarsh, A., Ariel, G., Schneidman, E., Ben-Jacob, E. (2011). Smart swarms of bacteria-inspired agents with performance adaptable interactions. *PLoS comp. bio.*, 7(9), e1002177.
3. Emek, Y., Wattenhofer, R. (2013, July). Stone age distributed computing. *In Proc. of the 2013 ACM symp. on Principles of distributed computing*, 137-146.
4. Lynch, N. A. (1996). Distributed algorithms. Morgan Kaufmann. Chapters 2-3.
5. Francis, K. and Palsson, B. O. (1997). Effective intercellular communication distances are determined by the relative time constants for cyto/chemokine secretion and diffusion. *Proceedings of the National Academy of Sciences*, 94(23), 12258-12262.
6. Taylor, Rion G., and Roy D. Welch. 'Chemotaxis as an emergent property of a swarm.' *Journal of bacteriology* 190.20 (2008): 6811-6816.